PV output power enhancement using two mitigation techniques for hot spots and partially shaded solar cells

Mahmoud Dhimish, Violeta Holmes, Bruce Mehrdadi, Mark Dales, Peter Mather

School of Computing and Engineering, University of Huddersfield, United Kingdom

Abstract

Hot spotting is a reliability problem in photovoltaic (PV) panels where a mismatched cell heats up significantly and degrades PV panel output power performance. High PV cell temperature due to hot spotting can damage the cell encapsulate and lead to second breakdown, where both cause permanent damage to the PV panel. Therefore, the design and development of two hot spot mitigation techniques are proposed using a simple, costless and reliable method. The hot spots in the examined PV system was carried out using FLIER i5 thermal imaging camera.

Several experiments have been examined during various environmental conditions, where the PV module I-V curve was evaluated in each observed test to analyze the output power performance before and after the activation of the proposed hot spot mitigation techniques. One PV module affected by hot spot was tested. The output power during high irradiance levels is increased by approximate to 1.25 W after the activation of the first hot spot mitigation technique. However, the second mitigation technique guarantee an increase of the power equals to 3.96 W. Additional test has been examined during partial shading condition. Both proposed techniques ensure a decrease in the shaded PV cell temperature, thus an increase in the output measured power.

Keywords: Hot spot protection; photovoltaic (PV) hot spotting analysis; solar cells; thermal imaging.

1. Introduction

Photovoltaic (PV) hot spots are a well-known phenomenon, described as early as in 1969 [1] and still present in PV modules [2 and 3]. PV hot spots occur when a cell, or group of cells, operates at reverse-bias, dissipating power instead of delivering it and, therefore, operating at abnormally high temperatures. This increase in the cells temperature will gradually degrade the output power generated by the PV module as explained by M. Simon & L. Meyer [4]. Hot spots are relatively frequent in current PV modules and this situation will likely persist as the PV module technology is evolving to thinner wafers, which are prone to developing micro-cracks during the manipulation process such as manufacturing, transportation and installation [5 and 6].

PV hot spots can be easily detected using IR inspection, which has become a common practice in current PV applications as shown in [7]. However, the impact of hot spots on operational efficiency and PV lifetime have been scarcely addressed, which helps to explain why there is lack of widely accepted procedures which deals with hot spots in practice as well as specific criteria referring to acceptance or rejection of affected PV module in commercial frameworks as described by R. Moretón et al [8]. Thus, this paper demonstrates two mitigation techniques which will improve the output power performance of the hot spotted PV modules.

39 In the past, the increase in the number of bypass diodes (up to one diode for each cell) has been
40 proposed as a possible solution [9 and 10]. However, this approach has not encountered the favor
41 of crystalline PV modules producers since it requires a not negligible technological cost and can
42 be even detrimental in terms of power production when many diodes are activated because of their
43 power consumption as discussed by S. Daliento et al [11].

44 In addition, the main prevention method for hot spotting is a passive bypass diode that is placed in
45 parallel with a string of PV cells. The use of bypass diodes across PV strings is standard practice
46 that is required is crystalline silicon PV panels [12 and 13]. Their purpose is to prevent hot spot
47 damage that can occur in series-connected PV cells [14]. Bypass diodes turn "on" to provide an
48 alternative current path and attempt to prevent extreme reverse voltage bias on PV strings. The
49 general misconception is that bypassing a string protects cells against hot spotting.

50 More recently, it has been shown that the distributed MPPT approach suggested by M. Coppola
51 [15] is beneficial for mitigating the hot spot in partially shaded modules with a temperature
52 reduction up to 20 ^{0}C for small shadows. On the other hand, [16 and 17] showing the
53 "inadequateness" of the standard bypass diode, the insertion of a series-connected switch are suited
54 to interrupt the current flow during bypass activation process. However, this solution requires a
55 quite complex electronic board design that needs devised power supply and suitable control logic
56 for activation the hot spot protection device.

57 A modified bypass circuit for improving the hot spot reliability of solar panels is proposed by S,
58 Daliento [18]. The technique relies on series-connected power MOSFET that subtracts part of the
59 reverse voltage from the shaded solar cell, thereby acting as a voltage divided, while the bypass
60 circuit does not require either a control logic or power supply and can be subtitled to the standard
61 bypass diodes of the PV panels.

62 This paper presents a simple solution for mitigating the impact of hot spots in PV solar cells. Two
63 techniques are proposed, where both hot spot mitigation techniques consists of multiple MOSTEFs
64 connected to the PV panel which is affected by a hot spot. Several experiments have been
65 examined during various environmental conditions, where the PV module I-V curve was evaluated
66 in each observed test to analyse the output power performance before and after the activation of
67 the proposed techniques.

68 One PV module affected by a hot spot was tested. After activating the first mitigation technique
69 the output power of the PV module increased by 1.25 W in high irradiance levels, 0.61 W in
70 medium irradiance level and 0.46 W in low irradiance level. Same experiments were carried out
71 using the 2nd proposed hot spot mitigation technique, while the output power increased by 3.96 W
72 in high irradiance levels, 2.72 in medium irradiance levels and 0.98 W in low irradiance levels.

73 The main contribution of this paper, is the development of a simple, reliable, and fast PV hot spot
74 mitigation technique which reduce the reverse voltage across hot spotted and shaded solar cells,
75 thus mitigating power dissipation and cell temperature. The approach is based on the adoption of
76 a low cost power MOSFETs that sustain part of the reverse voltage, therefore, dissipating a portion
77 of the power in the place of the shaded cells. Differently from [16, 20 and 21], the functioning
78 principle of the proposed approach does not require either power supply or control logic.

79 This paper is organized as follows: section 2 illustrates the examined PV system, while section 3
80 describes the proposed hot spot mitigation techniques. Section 4 shows the validation process of
81 the proposed hot spot mitigation techniques using two case studies. Lastly, section 5 demonstrates
82 the conclusion and the future work.

83 *2.   Photovoltaic System*

84 *2.1   Examined Photovoltaic Module Characteristics*

85 The PV system used in this work comprises a PV plant containing 9 polycrystalline silicon PV
86 modules each with a nominal power of 220 W_p. The SMT6 (60) P solar module manufactured by
87 Romag has been used in this work. The tilt angle of the PV installation is 42°. The electrical
88 characteristics of the solar module under standard test conditions (STC) are shown in Table 1. In
89 addition, Fig. 1(a) show the overall examined PV plant.

90 In order to examine the behavior of a PV module, it must be connected to a load. Otherwise, the
91 PV module would not generate an output power, since the PV module will be in open circuit mode.
92 In that case, it is only possible to measure the open circuit voltage and short circuit current.
93 Therefore, in this work, a resistive load was connected to the tested PV module through a
94 maximum power point tracking (MPPT) unit, which can be seen in Fig. 1(b).

95 The purpose of the MPPT unit is to track the maximum output power of the PV module under
96 various environmental conditions. The MPPT unit is manufactured by Outback Power. This unit
97 has a minimum output efficiency equals to 98.5% [19].

98 As can be noticed, the PV system does not contain a DC/AC inverter, since this work focuses on
99 the behavior of the PV modules in the DC side. Therefore, MPPT unit with resistive load was used
100 to test the reliability of the proposed methods.

101 Generally speaking, the performance of the DC/AC inverters used in PV systems are affected by
102 the input power of the PV modules in which it is affected by the PV module's temperature and
103 solar irradiance. Thus, the predictively of the performance for the inverters does not only depends
104 on the input power for the PV modules. Therefore, in this work we will be examining the
105 enhancement of the output power of PV modules under various environmental conditions, and it
106 is intended in the future to examine this improvement using an AC applications.

Table 1 Examined PV electrical characteristics

PV module electrical characteristics	Value
PV peak power	220 W
One PV cell peak power	3.6 W
Voltage at maximum power point (V_{mpp})	28.7 V
Current at maximum power point (I_{mpp})	7.67 A
Open Circuit Voltage (V_{oc})	36.74 V
Short Circuit Current (I_{sc})	8.24 A

3

107 I-V curve tracer was also used to plot the I-V curve of the examined PV modules under various
108 experimental conditions. The main specification, including the voltage resolution, and current
109 resolution can be seen in Fig. 1(b). As can be noticed, the error in the measured PV voltage, PV
110 current, solar irradiance and PV module temperature is very limited due to the high accuracy of
111 the I-V tracer, which approximately cost 4,500£.

112 The AC side of the PV installation has not been considered, since, this work focuses on the
113 behavior of the hot spotted PV modules. As stated in the introduction, there is a rapid decrease in
114 the output power for the hot spotted PV modules. Therefore, this work demonstrates two different
115 techniques to increase the reliability of the hot spotted PV modules, which will be described in
116 section 3.

(a)
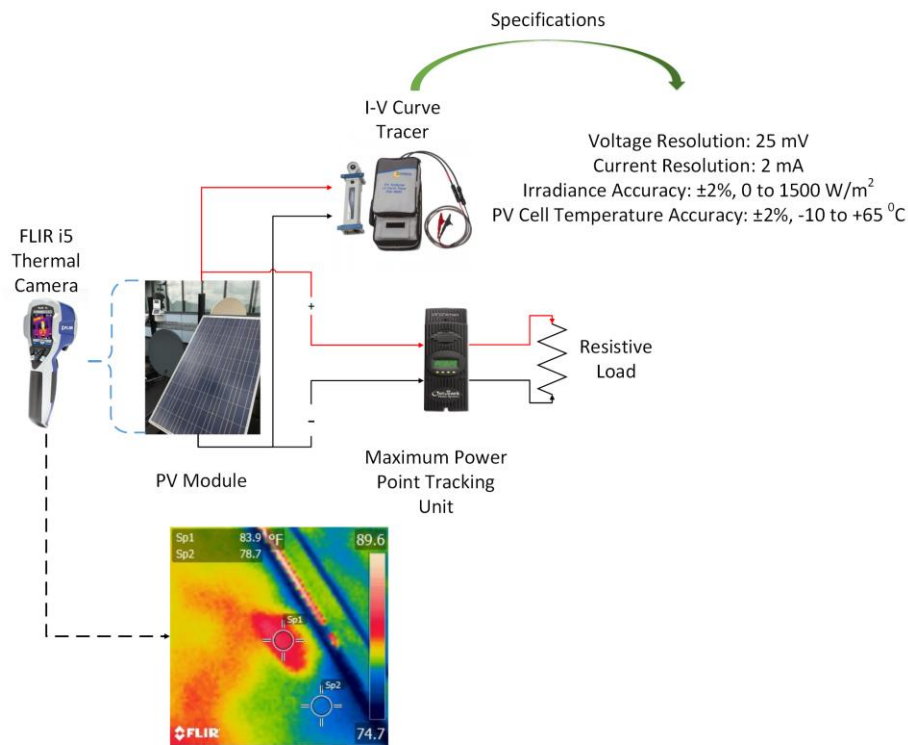
(b)

Fig. 1. (a) Examined PV system installed at the University of Huddersfield, United Kingdom,
(b) Structure and the used instruments to examine the hot spotted PV modules

4

117   *2.2   Evaluating the Photovoltaic I-V Curve Tracer and i5 FLIR Thermal Camera*

118   In this section, the output results of the I-V curve tracer shown previously in Fig. 1(b) will be
119   evaluated using various environmental conditions affecting a PV module.

120   Fig. 2 shows three different I-V curves experimented under high, medium, and low irradiance
121   levels. The theoretical maximum power point (MPP) and measured MPP at each environmental
122   condition is reported, where the accuracy of the I-V curve tracer is equal to:

123   1. High irradiance level: (185.60 / 186.382) x 100 = 99.58%
124   2. Medium irradiance level: (107.79 / 108.299) x 100 = 99.53%
125   3. Low irradiance level: (30.409 / 30.5991) x 100 = 99.38%

126   As can be seen, the accuracy of the measured MPP and I-V curves is nearly equal to the theoretical
127   data, where the average accuracy in all reported data in Fig. 2 is equal to 99.5%.

128   The investigation of the hot spots in the examined PV system was carried out using FLIR i5
129   thermal camera as shown in Fig. 1(b). This camera has a thermal sensitivity equals to 32.18 ^{0}F,
130   where its specification is reported in Table 2.
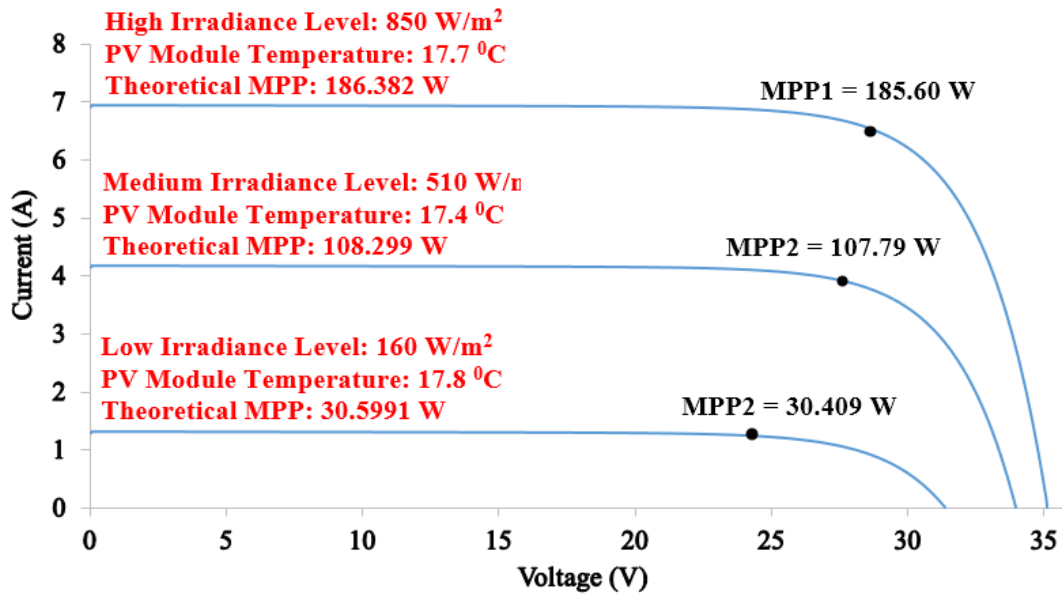

Fig. 2. I-V curve tracer output results for various irradiance levels

Table 2 FLIR i5 camera specification

| Comparison	Value
Thermal image quality	100x100 pixels
Field of view	21^0 (H) x 21^0 (V)
Thermal sensitivity	32.18 ^{0}F

131 Another test was carried out using a PV module affected by one hot spotted solar cell. The thermal
132 image of the examined PV module is shown in Fig. 3(a). As can be seen, the temperature of the
133 hot spotted solar cell is equal to 66.3 F, however, the temperature of the adjacent solar cells are
134 between 60.1 and 57.7 ^{0}F.

135 The I-V curve of the hot spotted PV module is compared with healthy PV module (PV module
136 without hot spots). The results is shown in Fig. 3(b). The MPP for a PV module without hot spot
137 is equal to 121.61 W. However, the MPP for hot spotted PV module is equal to 115.83 W.
138 Therefore, the power loss due to the hot spot in the examined PV module is equal to 5.78 W.

139 This experiment was carried out under 621 W/m^2 solar irradiance and the PV modules temperature
140 is approximately equal to 18.2 ^{0}C. Furthermore, according to the measured data in Fig. 2, the
141 average accuracy of the I-V curve tracer is equal to 99.5%. Therefore, the measured data illustrated
142 in Fig. 3(b) has an error in the measurements equals to ±0.5%.
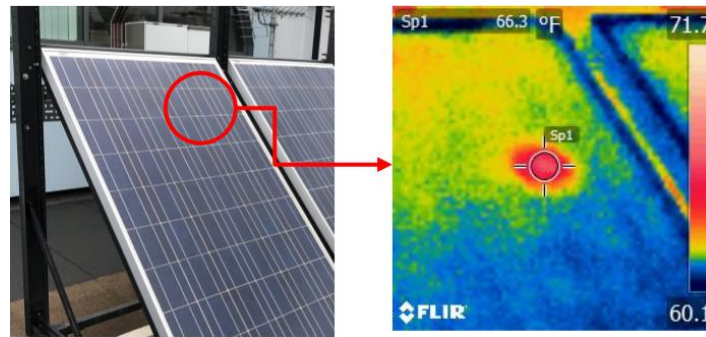
(a)
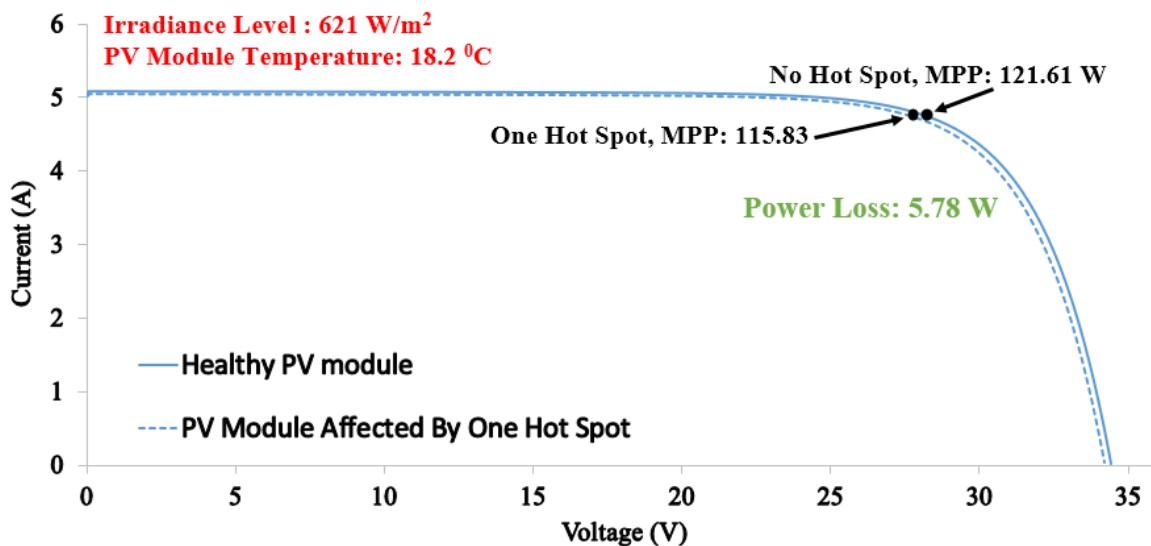
(b)

Fig. 3. (a) Hot Spot detection using FLIR thermal camera, (b) Output results using healthy PV
module vs. the hot spotted PV module

6

143 *3.   **Proposed Hot Spot Mitigation Techniques***

144 The first proposed hot spot mitigation technique is connected to each PV string in the PV module.
145 As can be seen in Fig. 4(a), the examined PV module used in this work contains three sub strings
146 connected throw bypass diodes.

147 In order to apply the proposed hot spot protection system, two MOSFETs were connected to each
148 PV string as shown in Fig. 4(b). Switch 1 is in series with the PV string and is normally "on"; it
149 opens when a hot spot condition is detected to prevent further hot spotting. While, switch 2 is in
150 parallel with the PV string and it is normally in "open" mode, it turns "on" to allow a bypass
151 current path when the PV string is open circuited.

152 Another hot spot mitigation technique was used with the PV module instead of the connection for
153 each MOSFET to the PV strings as shown in Fig. 4(c). The same concept has been applied, where
154 switch 1 is in series with the PV module is normally "on"; it opens when a hot spot condition is
155 detected to prevent further hot spotting. Switch 2 is in parallel with the PV module and is normally
156 "open"; it turn "on" to allow a bypass current path when the PV string is open circuited. The two
157 switch PV protection device has been implemented and connected to the PV panel which contains
158 the hot spot.

159 As can be noticed, the proposed techniques are simple to implement, where the connection steps
160 is also within the PV module limit, since it requires only to add additional MOSFETs to the hot
161 spotted PV module.

162 Moreover, Power MOSFETs IRFZ44V were used to implement and test the suggested hot spot
163 mitigation techniques. The MOSFETs drain-to-source breakdown voltage is equal to 60 V, and
164 the voltage drop in drain-to-source as low as 50 mV. Hence, the selection of the MOSFETs plays
165 an important role in the mitigation techniques, therefore, the following MOSFET criteria must be
166 met (any other MOSFET meet these criteria can be used to implement the suggested hot spot
167 mitigation techniques):

168   1. Low drain-to-source voltage drop: better results in the I-V curve

169   2. Fast switching speed: to enable fast drop in the temperature of the hot spotted solar cell

170   3. Low on-resistance: low resistance means more current passes through the PV string

171   4. High operating temperature

172   5. Cost effective – for industrial applicability

173 The cost of the used MOSFETs is equal to 0.85£. Therefore, the total cost for the first and second
174 presented techniques using 3 PV modules are equal to 18£ and 5.1£ respectively.

175 In the next section, the validation and comparison between both presented hot spot mitigation
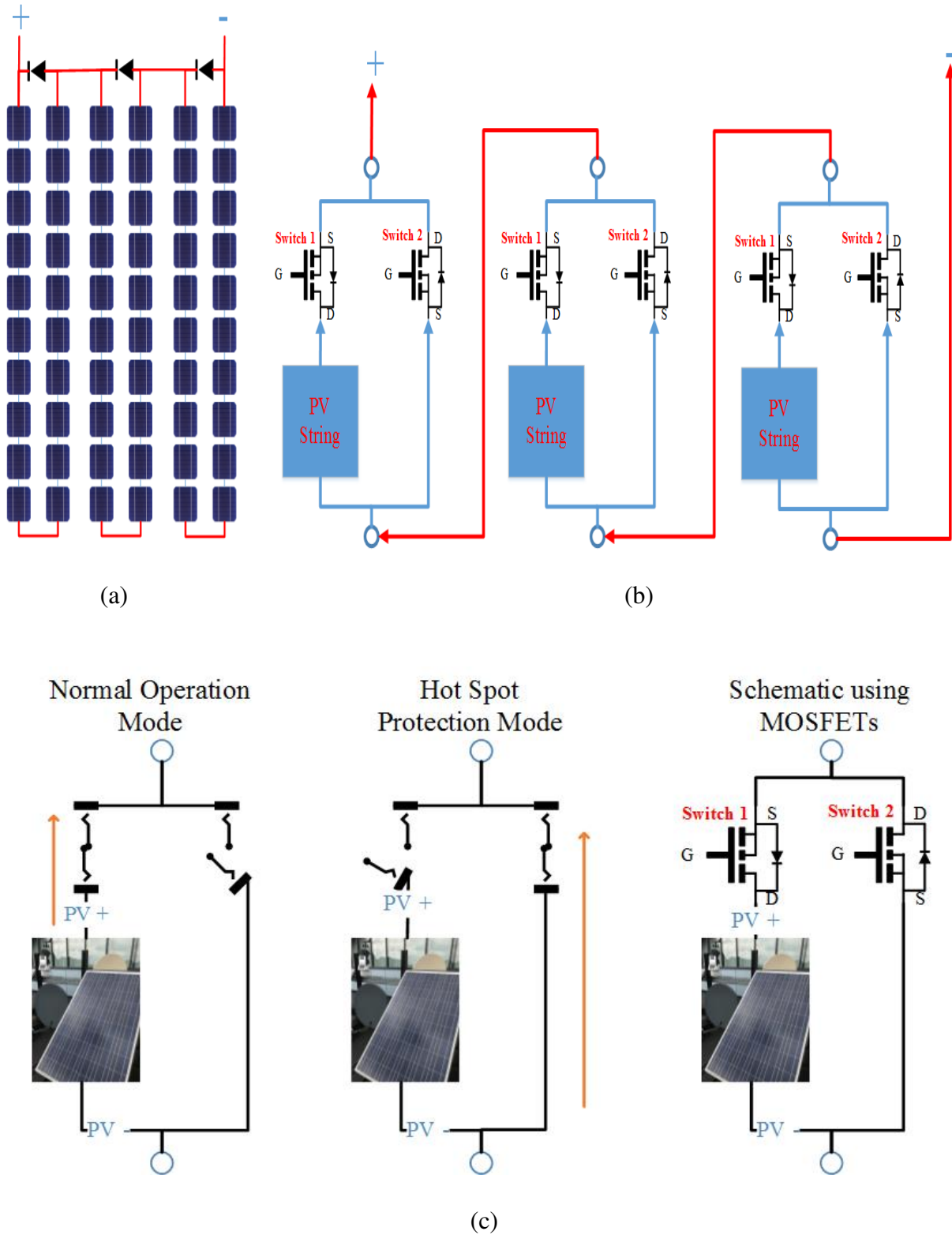176 techniques are illustrated in brief.

Fig. 4. (a) The structure of the PV string for the examined PV module, (b) First hot spot mitigation technique, (c) Second proposed hot spot mitigation technique

178   *4.   Validation of the Proposed Hot Spot Protection Method*

179   In this section the validation for both proposed hot spot mitigation techniques are demonstrated
180   and compared. The output power has been carried out using the analysis of the I-V curve of the
181   examined PV module, where the detection of the hot spot has been captured using FLIR i5 camera.

182   *4.1   Photovoltaic Hot Spot and I-V Curve Analysis*

183   The proposed hot spotting techniques were tested in an experimental setup with a resistive load
184   powered by the PV module which contains the hot spot, previously shown in Fig. 2, where the
185   MOSFETs are placed in the examined PV module as illustrated in Fig. 4(b) and Fig. 4(c).

186   There are several stages that have been assessed during the operation of the proposed hot spotting
187   mitigation technique, these stages are describes as follows:

188   **1. Hot spot mitigation technique 1:**

189   The results obtained by the first mitigation technique is shown in Fig. 5(a), the results can be
190   described by the following:

191   A. Before the activation: the temperature of the hot spotted PV solar cell is equal to 70 ^{0}F,
192   while the adjacent (reference) solar cells temperature is equal to 61.5 ^{0}F.
193   B. 1 minute after the activation: the temperature of the hot spotted PV solar cell reduced
194   to 68.7 ^{0}F, the difference between the hot spotted PV solar cell and the reference solar
195   cell temperature is equal to 7.2 ^{0}F.
196   C. 2 minutes after the activation: the maximum enhancement of the temperature for the
197   hot spotted PV solar cell is reduced to 67.1 ^{0}F, comparing to 70 ^{0}F before the activation
198   of the mitigation technique.
199
200   **2. Hot spot mitigation technique2:**

201   The results obtained by the first mitigation technique is shown in Fig. 5(b), the results can be
202   described by the following:

203   A. Before the activation: the temperature of the hot spotted PV solar cell is equal to 70.6
204   ^{0}F, while the adjacent (reference) solar cells temperature is equal to 61.8 ^{0}F.
205   B. 1 minute after the activation: the temperature of the hot spotted PV solar cell reduced
206   to 66.3 ^{0}F, the difference between the hot spotted PV solar cell and the reference solar
207   cell temperature is equal to 4.5 ^{0}F.
208   C. 2 minutes after the activation: the maximum enhancement of the temperature for the
209   hot spotted PV solar cell is reduced to 64.9 ^{0}F, comparing to 70.6 ^{0}F before the
210   activation of the mitigation technique.

211   As can be noticed, the obtained results for the hot spot mitigation technique 2 has a better
212   performance comparing to technique 1, where the maximum difference between the hot spotted
213   PV solar cell and the adjacent solar cells is equal to 3.1 ^{0}F.
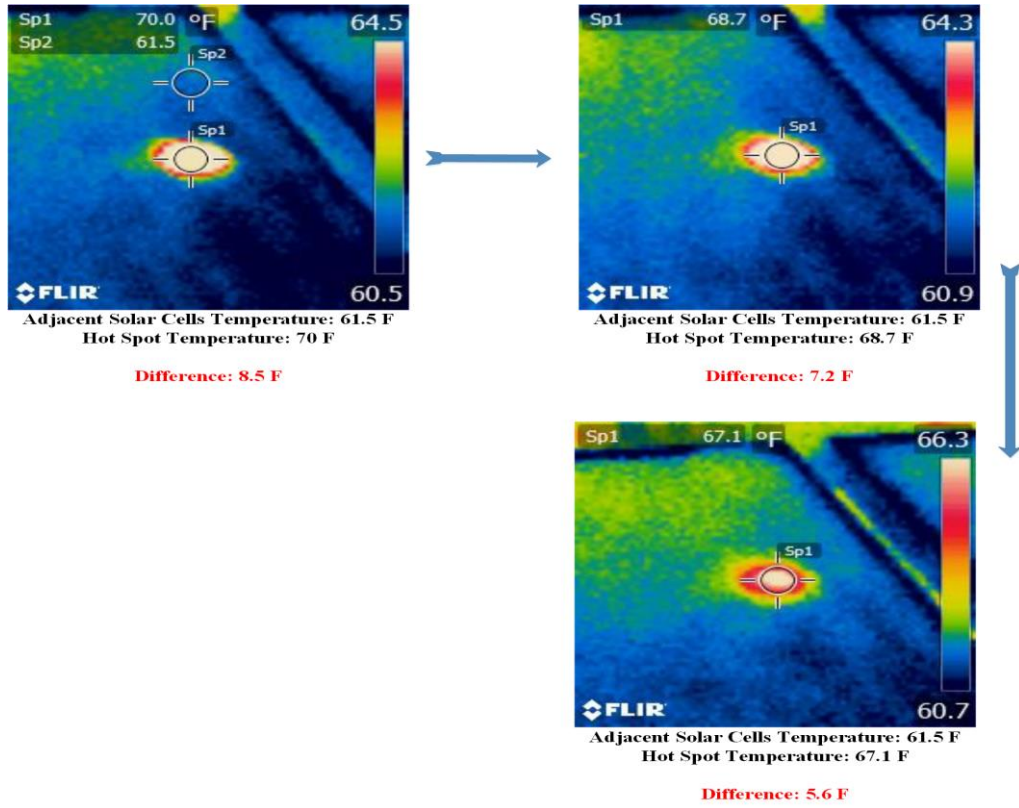
(a)
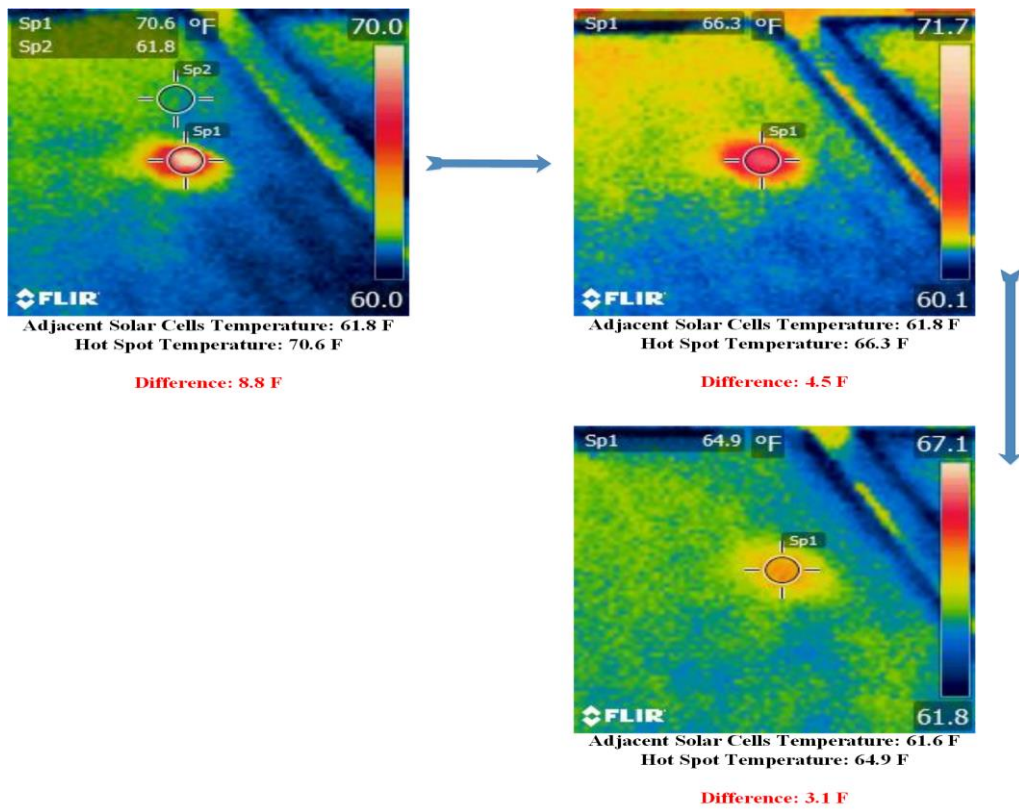
(b)

Fig. 5. (a) Output thermal images the first for hot spot mitigation technique, (b) Output thermal images for the second hot spot mitigation technique

215 The main reason for the proposed hot spotting mitigation techniques is to improve the output power
216 performance of the examined hot spotted PV module. The value of the power before and after the
217 activation for each proposed technique was monitored in three different irradiance levels: high
218 irradiance level: 840 W/m^2, medium irradiance level: 507 W/m^2 and low irradiance level: 177
219 W/m^2, while in all tested scenarios, the PV temperature is approximately equal to 16.2 $^{\circ}$C.

220 Fig. 6(a) shows the output I-V curve of the PV module at high irradiance level. The measured
221 output power after the activation of the proposed 1st technique has a power loss equals to 3.94 W
222 comparing to 5.19 W with no mitigation technique deployed in the PV module. However, the
223 minimum loss in the output power is estimated while activating the 2nd hot spot mitigation
224 technique (P_{loss} = 1.23 W). A brief comparison between both examined techniques are shown in
225 Table 3.

226 The output I-V curve of the examined PV module under medium and low irradiance levels are
227 shown in Fig. 6(b) and Fig. 6(c) respectively. The output results show a significant improvement
228 in the output power of the 2nd mitigation technique comparing to the 1st technique. Table 3
229 demonstrates a comparison between the output results in each examined irradiance level.

230 In conclusion, this section shows the validation and the enhancement of the temperature and the
231 output power generated by the PV module using both proposed hot spot mitigation techniques.
232 Additionally, technique 2 has a better output power performance comparing to the 1st proposed
233 mitigation technique.

Table 3 Comparison between the first and second proposed hot spot mitigation technique using high, medium and low irradiance levels

Irradiance (W/m^2)	Theoretical Power (W)	Case Scenario	Voltage (V)	Current (A)	Power (W)	P_{loss} (W)	Efficiency (%)
High 840	186.4	No mitigation	27.19	6.66	181.18	5.19	97.2
		1st Technique	27.49	6.63	182.44	3.94	97.88
		2nd Technique	28.33	6.53	185.15	1.23	99.33
Medium 507	108.2	No mitigation	26.00	4.02	104.54	3.63	96.64
		1st Technique	26.23	4.00	105.15	3.02	97.20
		2nd Technique	27.21	3.94	107.26	0.91	99.15
Low 177	34.4	No mitigation	23.73	1.39	33.02	1.37	95.99
		1st Technique	24.24	1.38	33.49	0.91	97.33
		2nd Technique	24.94	1.36	34.01	0.39	98.85
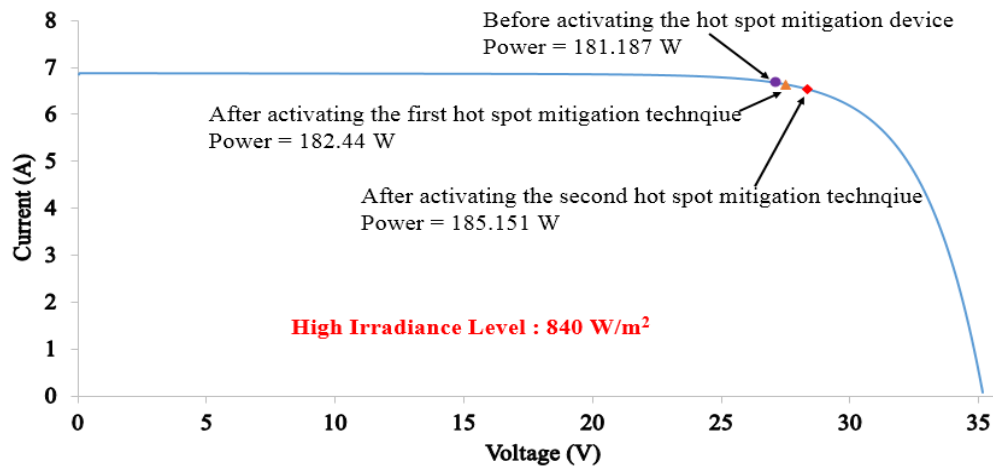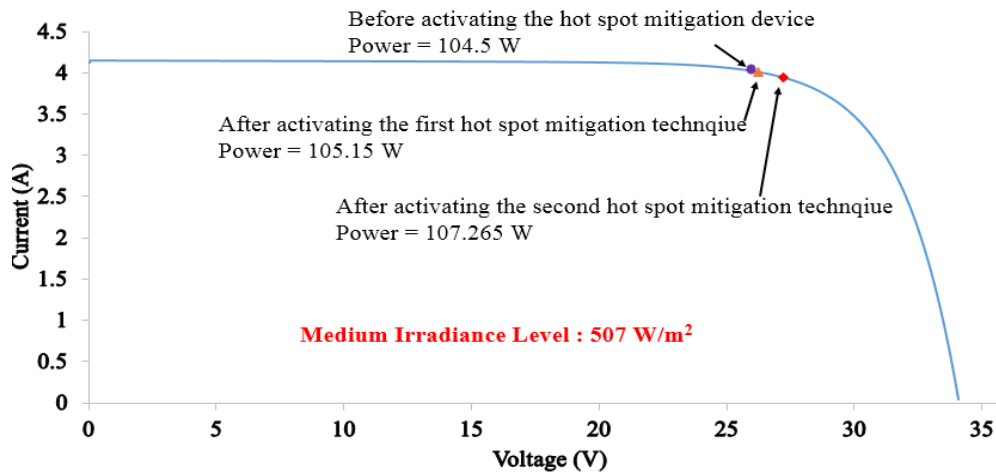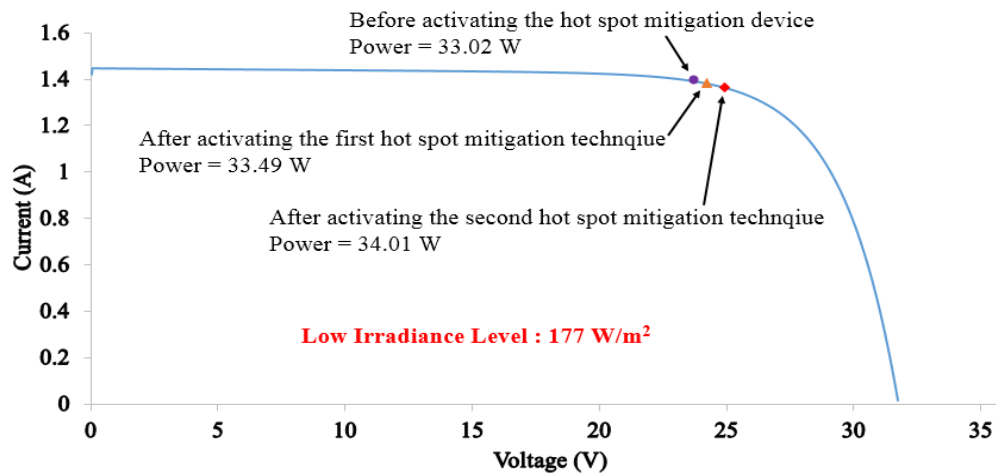
Fig. 6. Photovoltaic I-V curve. (a) Before and after considering hot spot mitigation techniques at G: 840 W/m², (b) Before and after considering hot spot mitigation techniques at G: 507 W/m², (c) Before and after considering hot spot mitigation techniques at G: 177 W/m²

235   *4.2   Photovoltaic Partial Shading Analysis*

236   The main purpose of this section is to test the ability of the proposed hot spot mitigation techniques
237   to increase the output power of a PV module during partial shading conditions affecting any PV
238   module. PV Partial shading has been introduced by many researches such as [22 - 25], where there
239   is a limited results which includes the mitigation of the temperature of the shades solar cell.

240   In order to test the ability of the proposed hot spot mitigation techniques, another experimental test
241   has been carried out on a PV module with partially shaded solar cell. Fig. 7 shows an image of the
242   examined PV module under shaded solar cell using paper opaque object. The PV module was
243   experimented under the same irradiance level which is equal to 784 W/m^2. Moreover, in each
244   tested experiment the temperature of the shaded solar cell was captured using the FLIR i5 camera.

245   The first test was carried out using the activation of the first proposed hot spot mitigation
246   technique. Fig. 8(a) shows the thermography image of the shaded solar cell before and after the
247   activation of the 1st hot spot mitigation technique. Before the activation, the temperature of the
248   shaded solar cell is equal to 66.6 ^{0}F. The solar cell temperature decreases to a minimum value of
249   63.9 ^{0}F after the activation of the hot spot mitigation technique. This decrease in the value of the
250   temperature will guarantee an increase in the output power produced by the PV module. As
251   illustrated in Fig. 9(a), the output power before and after the activation is equal to 171.787 W and
252   172.508 W respectively. Thus, the total increase in the output power is equal to 0.721 W.

253   The second test was tested using the activating of the second proposed hot spot mitigation
254   technique. Fig. 8(b) displays the thermal images of the examined shaded solar cell before and after
255   activating the mitigation technique. The difference in the temperature of the shaded solar cell is
256   equal to:

257   (No mitigation) 71.0 ^{0}F – (After activating the 2nd hot spot mitigation technique) 65.3 ^{0}F = 5.7 ^{0}F

258   In addition, this decrease in the temperature of the shaded solar cell guarantee an increase of the
259   measured maximum power point of the PV module. Fig. 9(b) describes that the total increase in
260   the output measured power is equal to 1.689 W.

261   In conclusion, this section demonstrates that both proposed hot spot mitigation techniques are
262   useful in case a partial shading conditions have been occurred in the PV module. An enhancement
263   of the temperature and output power of the PV module is guaranteed. Furthermore, the second
264   proposed hot spot mitigation technique shows better performance comparing to the 1st technique.

Fig. 7. Image of the tested PV module under shaded solar cell using paper opaque object
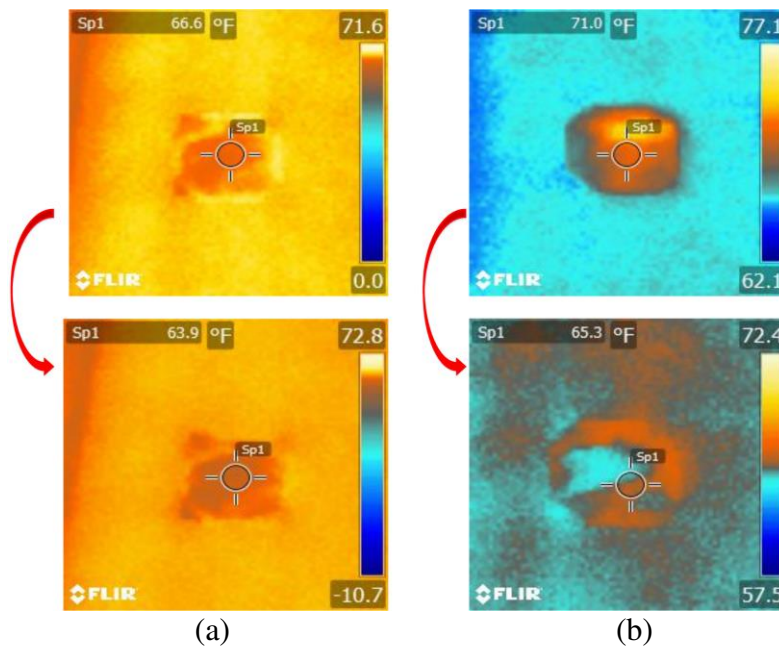
(a)   (b)

Fig. 8. (a) Thermographic images of the shaded PV solar cell before and after the activation of the first hot spot mitigation technique, (b) Thermographic images of the shaded PV solar cell before and after the activation of the second hot spot mitigation technique
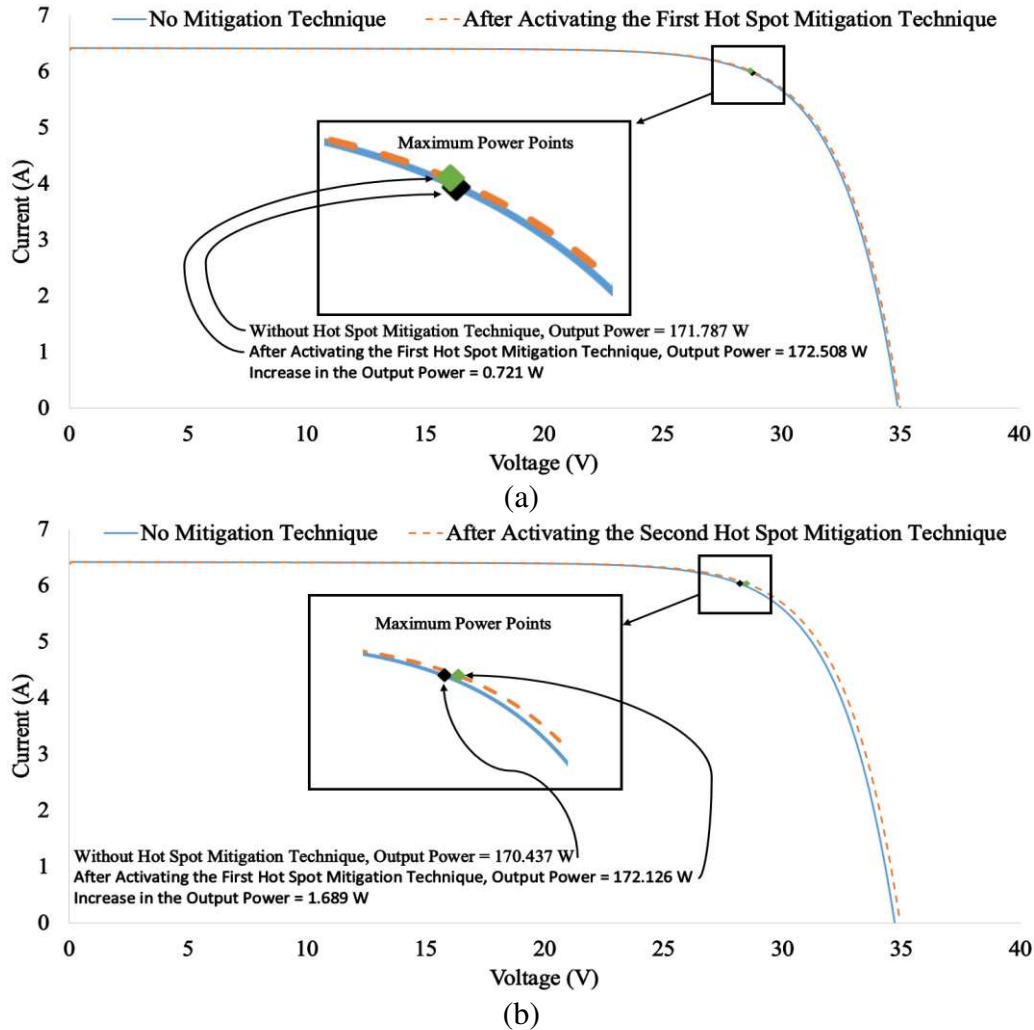

(a)

(b)

Fig. 9. Photovoltaic output I-V curve. (a) Before and after activating the first hot spot mitigation technique, (b) before and after activating the second hot spot mitigation technique

14

266   *5.   Conclusion*

267   In this paper, the design and development of two hot spot mitigation techniques are proposed. The
268   offered techniques are capable to enhance the output power of PV modules which are effected by
269   hot spots and partial shading conditions. Both techniques use multiple MOSFTEs in the affected
270   PV module, while the detection of hot spots was captured using i5 FLIR thermal imaging camera.

271   Several experiments have been examined during various environmental conditions, where the PV
272   module I-V curve was evaluated in each observed test to analyze the output power performance
273   before and after the activation of both proposed hot spot mitigation techniques.

274   One PV module affected by a hot spot was tested. After activating the first mitigation technique
275   the output power of the PV module increased by 1.25 W in high irradiance levels, 0.61 W in
276   medium irradiance level and 0.46 W in low irradiance level. Same experiments have been
277   evaluated using the 2nd proposed hot spot mitigation technique, while the output power increased
278   by 3.96 W in high irradiance level, 2.72 W in medium irradiance level and 0.98 W in low irradiance
279   level.

280   Additionally, both proposed hot spot mitigation techniques were applied on a shaded PV module.
281   The temperature and output power of the PV module enhanced using both techniques, however,
282   the second mitigation technique shows a better performance comparing to the 1st.

283   In future, it is intended to improve the hot spot mitigation techniques to work with several PV
284   array configuration systems. In addition, the techniques could be improved to enhance the output
285   power of micro-cracked PV modules.

286   *6.   References*

287   [1]   Blake, F. A., & Hanson, K. L. (1969, August). The hot-spot failure mode for solar arrays.
288   In *Proceedings of the 4th Intersociety Energy Conversion Engineering Conference* (pp.
289   575-581).

290   [2]   Dhimish, M., Holmes, V., Mehrdadi, B., Dales, M., Chong, B., & Zhang, L. (2017). Seven
291   indicators variations for multiple PV array configurations under partial shading and faulty
292   PV conditions. *Renewable Energy*.

293   [3]   Orduz, R., Solórzano, J., Egido, M. Á., & Román, E. (2013). Analytical study and
294   evaluation results of power optimizers for distributed power conditioning in photovoltaic
295   arrays. *Progress in Photovoltaics: Research and Applications*, *21*(3), 359-373.

296   [4]   Simon, M., & Meyer, E. L. (2010). Detection and analysis of hot-spot formation in solar
297   cells. *Solar Energy Materials and Solar Cells*, *94*(2), 106-113.

298   [5]   Chaturvedi, P., Hoex, B., & Walsh, T. M. (2013). Broken metal fingers in silicon wafer
299   solar cells and PV modules. *Solar Energy Materials and Solar Cells*, *108*, 78-81.

300   [6]   M. Dhimish, V. Holmes, B. Mehrdadi, M. Dales, The Impact of Cracks on Photovoltaic
301   Power Performance, *Journal of Science: Advanced Materials and Devices* (2017), doi:
302   10.1016/j.jsamd.2017.05.005.

[7]   Buerhop, C., Schlegel, D., Niess, M., Vodermayer, C., Weißmann, R., & Brabec, C. J. (2012). Reliability of IR-imaging of PV-plants under operating conditions. *Solar Energy Materials and Solar Cells*, *107*, 154-164.

[8]   Moretón, R., Lorenzo, E., & Narvarte, L. (2015). Experimental observations on hot-spots and derived acceptance/rejection criteria. *Solar energy*, *118*, 28-40.

[9]   Hasyim, E. S., Wenham, S. R., & Green, M. A. (1986). Shadow tolerance of modules incorporating integral bypass diode solar cells. *Solar cells*, *19*(2), 109-122.

[10]   Chen, K., Chen, D., Zhu, Y., & Shen, H. (2012). Study of crystalline silicon solar cells with integrated bypass diodes. *Science China Technological Sciences*, *55*(3), 594-599.

[11]   Daliento, S., Mele, L., Bobeico, E., Lancellotti, L., & Morvillo, P. (2007). Analytical modelling and minority current measurements for the determination of the emitter surface recombination velocity in silicon solar cells. *Solar energy materials and solar cells*, *91*(8), 707-713.

[12]   Dhimish, M., & Holmes, V. (2016). Fault detection algorithm for grid-connected photovoltaic plants. *Solar Energy*, *137*, 236-245.

[13]   Silvestre, S., Boronat, A., & Chouder, A. (2009). Study of bypass diodes configuration on PV modules. *Applied Energy*, *86*(9), 1632-1640.

[14]   Dhimish, M., Holmes, V., Mehrdadi, B., & Dales, M. (2017). Diagnostic method for photovoltaic systems based on six layer detection algorithm. *Electric Power Systems Research*, *151*, 26-39.

[15]   Coppola, M., Daliento, S., Guerriero, P., Lauria, D., & Napoli, E. (2012, June). On the design and the control of a coupled-inductors boost dc-ac converter for an individual PV panel. In *Power Electronics, Electrical Drives, Automation and Motion (SPEEDAM), 2012 International Symposium on* (pp. 1154-1159). IEEE.

[16]   Kim, K. A., & Krein, P. T. (2015). Reexamination of photovoltaic hot spotting to show inadequacy of the bypass diode. *IEEE Journal of Photovoltaics*, *5*(5), 1435-1441.

[17]   d'Alessandro, V., Guerriero, P., Daliento, S., & Gargiulo, M. (2011). A straightforward method to extract the shunt resistance of photovoltaic cells from current–voltage characteristics of mounted arrays. *Solid-State Electronics*, *63*(1), 130-136.

[18]   Daliento, S., Di Napoli, F., Guerriero, P., & d'Alessandro, V. (2016). A modified bypass circuit for improved hot spot reliability of solar panels subject to partial shading. *Solar Energy*, *134*, 211-218.

[19]   M. Dhimish, V. Holmes, M. Dales, Parallel fault detection algorithm for grid-connected photovoltaic plants, Renewable Energy (2017), doi: 10.1016/j.renene.2017.05.084.

[20]   Solórzano, J., & Egido, M. A. (2014). Hot-spot mitigation in PV arrays with distributed MPPT (DMPPT). *Solar Energy*, *101*, 131-137.

339   [21]   Dhimish, M., Holmes, V., Mehrdadi, B., Dales, M., & Mather, P. (2017). Photovoltaic fault
340   detection algorithm based on theoretical curves modelling and fuzzy classification system.
341   *Energy*, *140*, 276-290.

342   [22]   Çelik, Ö., & Teke, A. (2017). A Hybrid MPPT method for grid connected photovoltaic
343   systems under rapidly changing atmospheric conditions. *Electric Power Systems Research*,
344   *152*, 194-210.

345   [23]   Khalid, M. S., & Abido, M. A. (2014). A novel and accurate photovoltaic simulator based
346   on seven-parameter model. *Electric Power Systems Research*, *116*, 243-251.

347   [24]   Dhimish, M., Holmes, V., Mehrdadi, B., & Dales, M. (2017). Simultaneous fault detection
348   algorithm for grid-connected photovoltaic plants. *IET Renewable Power Generation*,
349   *11*(12), 1565-1575.

350   [25]   Dhimish, M., Holmes, V., Mehrdadi, B., & Dales, M. (2018). Comparing Mamdani Sugeno
351   fuzzy logic and RBF ANN network for PV fault detection. Renewable Energy, 117, 257-
352   274.